The Plant Cell, Vol. 22: 3053–3065, September 2010, www.plantcell.org © 2010 American Society of Plant Biologists

The *Arabidopsis* Exocyst Complex Is Involved in Cytokinesis and Cell Plate Maturation

Matyáš Fendrych,[a] Lukáš Synek,[a] Tamara Pečenková,[a,b] Hana Toupalová,[a] Rex Cole,[c] Edita Drdová,[a] Jana Nebesářová,[d,e] Miroslava Šedinová,[f] Michal Hála,[a] John E. Fowler,[c] and Viktor Žárský[a,b,1]

[a] Institute of Experimental Botany, Academy of Sciences of the Czech Republic, 165 02 Prague 6, Czech Republic
[b] Department of Plant Physiology, Faculty of Science, Charles University, 128 44 Prague 2, Czech Republic
[c] Department of Botany and Plant Pathology and Center for Genome Research and Biocomputing, Oregon State University, Corvallis, Oregon 97331
[d] Biology Centre of ASCR, Institute of Parasitology, 370 05 České Budějovice, Czech Republic
[e] Laboratory of Electron Microscopy, Faculty of Science, Charles University, 128 44 Prague 2, Czech Republic
[f] Laboratory of Mass Spectrometry, Faculty of Science, Charles University, 128 44 Prague 2, Czech Republic

Cell reproduction is a complex process involving whole cell structures and machineries in space and time, resulting in regulated distribution of endomembranes, organelles, and genomes between daughter cells. Secretory pathways supported by the activity of the Golgi apparatus play a crucial role in cytokinesis in plants. From the onset of phragmoplast initiation to the maturation of the cell plate, delivery of secretory vesicles is necessary to sustain successful daughter cell separation. Tethering of secretory vesicles at the plasma membrane is mediated by the evolutionarily conserved octameric exocyst complex. Using proteomic and cytologic approaches, we show that EXO84b is a subunit of the plant exocyst. *Arabidopsis thaliana* mutants for *EXO84b* are severely dwarfed and have compromised leaf epidermal cell and guard cell division. During cytokinesis, green fluorescent protein–tagged exocyst subunits SEC6, SEC8, SEC15b, EXO70A1, and EXO84b exhibit distinctive localization maxima at cell plate initiation and cell plate maturation, stages with a high demand for vesicle fusion. Finally, we present data indicating a defect in cell plate assembly in the *exo70A1* mutant. We conclude that the exocyst complex is involved in secretory processes during cytokinesis in *Arabidopsis* cells, notably in cell plate initiation, cell plate maturation, and formation of new primary cell wall.

INTRODUCTION

Plant cells live interconnected by cell walls that define their shapes. The ability to form cell walls depends on delivery of new cell wall material, membrane components, and extracellular proteins to precisely defined locations in the cell cortex, closely interacting with adjacent endomembrane compartments. Such exocytotically active plasma membrane regions (also referred to as activated cortical domains; for a review, see Žárský et al., 2009) are delimited by a complex array of cytoskeletal and membrane-associated proteins.

Across the eukaryotes, evidence indicates that secretory vesicles can be tethered to the plasma membrane by the exocyst, a heterooligomeric protein complex. Based on findings in the budding yeast, the exocyst acts prior to SNARE (soluble *N*-ethylmaleimide–sensitive attachment protein receptors) assembly and together with small G-proteins of the Rab and Rho families confers spatial specificity to the membrane fusion (Guo et al., 1999b, 2001; Grote et al., 2000; Zhang et al., 2001). The exocyst localizes to sites of active secretion, such as the emerging bud in yeast (TerBush and Novick, 1995) or growing neurite in mammals (Hazuka et al., 1999). In yeast and mammals, the exocyst consists of eight subunits, SEC3, SEC5, SEC6, SEC8, SEC10, SEC15, EXO70, and EXO84 (TerBush et al., 1996; Hsu et al., 1998; Guo et al., 1999a). The assembly of exocyst subunits has been hypothesized to integrate information from various regulators and to act as a hub controlling membrane fusion (Zajac et al., 2005).

Plants possess homologs of all exocyst subunits (Eliáš et al., 2003); most of them, unlike those of fungi or mammals, are encoded by two or more paralogous genes, the extreme example being EXO70, encoded by a family of 23 genes in *Arabidopsis thaliana* (Synek et al., 2006). Recently, the presence of the exocyst as a complex in plants was confirmed, and its importance for plant development and cell morphogenesis was demonstrated in *Arabidopsis* (Hála et al., 2008). *Arabidopsis exo70A1* mutants lacking the most abundantly expressed EXO70 isoform display multiple defects, such as abnormal plant architecture, retarded polar cell growth, and reduced cell number in many organs (Synek et al., 2006). Mutants in other exocyst subunits exhibit defects in germination and tip growth of pollen tubes (Cole et al., 2005; Hála et al., 2008). Similarly, a mutation in maize (*Zea mays*) *SEC3* homolog *RTH1* results in short root hairs and small stature of homozygous mutants (Wen et al., 2005). The

[1] Address correspondence to zarsky@ueb.cas.cz.
The author responsible for distribution of materials integral to the findings presented in this article in accordance with the policy described in the Instructions for Authors (www.plantcell.org) is: Viktor Žárský (zarsky@ueb.cas.cz).
www.plantcell.org/cgi/doi/10.1105/tpc.110.074351

exocyst was also revealed to be crucial for seed coat development (Kulich et al., 2010) and pollen–pistil interaction (Samuel et al., 2009). The study of plant exocyst regulators is only beginning; however, Lavy et al. (2007) demonstrated that the SEC3 subunit interacts with plant-specific Rho GTPases via an adaptor protein ICR1 in *Arabidopsis*.

Similarly to the situation in plants (Hála et al., 2008), the original description of the yeast exocyst complex did not document Exo84 (TerBush et al., 1996). In yeast, it was later discovered as a subunit by coimmunoprecipitation with the remaining subunits (Guo et al., 1999a). Electron microscopy and analyses of cargo protein trafficking in yeast *exo84* mutants indicated that Exo84 is involved in the post-Golgi stage of secretion (Zhang et al., 2005b). The same study demonstrated that Exo84 plays a critical role in both the assembly of the exocyst and its targeting to sites of secretion. The crystal structure of the C terminus of yeast Exo84 revealed that the protein forms a long rod, exhibiting a novel fold shared among exocyst subunits (Dong et al., 2005; Wu et al., 2005; Hamburger et al., 2006; Sivaram et al., 2006; Croteau et al., 2009).

In addition to the role in plant cell growth, the exocyst has been hypothesized to participate in cytokinesis in plants. During cell plate formation in *Arabidopsis* cells, exocyst-like structures connecting vesicles were observed by electron tomography (Otegui and Staehelin, 2004; Seguí-Simarro et al., 2004; Otegui et al., 2005). Plant cytokinesis strictly depends on the proper functioning of targeted secretion to generate new plasma membrane (Samuels et al., 1995; Verma, 2001; Jürgens, 2005). In late anaphase, a plant-specific cytoskeletal and endomembrane array, the phragmoplast, is assembled. Vesicle fusion occurs inside this structure, giving rise to the cell plate, a transient membrane compartment that grows centrifugally by membrane remodeling and by further vesicle fusion at the cell plate periphery. Eventually, the cell plate inserts into the mother cell plasma membrane. The insertion triggers the maturation of the cell plate, resulting in the establishment of a postcytokinetic primary cell wall between the two daughter cells (Samuels et al., 1995; Otegui et al., 2001; Seguí-Simarro et al., 2004).

The role of the exocyst complex in cytokinesis has been shown in several nonplant systems. In *Saccharomyces cerevisiae*, the exocyst localizes to the bud neck between the mother and daughter cells (Finger et al., 1998). In *Schizosaccharomyces pombe*, the exocyst is necessary for abscission and localizes to the abscission site (Wang et al., 2002). In mammalian cells, the exocyst was proposed to be anchored in the midbody by centriolin and was shown to be essential for abscission (Gromley et al., 2005).

Here, we provide experimental data demonstrating that EXO84 is a subunit of the *Arabidopsis* exocyst complex. In addition, we show that mutants defective in *EXO84b* exhibit a dwarf phenotype with cytokinetic defects. Finally, EXO84b and exocyst subunits SEC6, SEC8, SEC15b, and EXO70A1 all localize distinctly to the nascent cell plate and later to the cell plate insertion site and along the postcytokinetic wall. Finally, *exo70A1* mutants are associated with an aberrant initial stage of cell plate formation. These data suggest that EXO84b and the exocyst participate in cytokinesis in *Arabidopsis*.

RESULTS

EXO84 Is Part of the *Arabidopsis* Exocyst Complex

The *Arabidopsis* genome encodes three *EXO84* paralogs (Eliáš et al., 2003). We focused our work mainly on *EXO84b* as the only paralog whose mutation produced a readily discernible developmental phenotype (see below). We previously reported that the full-length EXO84b strongly autoactivates the reporter genes in the GAL4-based yeast two-hybrid system, thus hampering analysis of its interactors (Hála et al., 2008). To overcome this, we prepared constructs derived from N- and C-terminal domains of EXO84b to test its interactions with other exocyst subunits. The N-terminal domain strongly interacted with EXO70A1 both as bait and prey and weakly interacted as bait with SEC15b. On the other hand, the C-terminal domain of EXO84b exhibited weak interactions with itself and, as bait, with SEC15b (Figure 1A).

We further demonstrated the association of EXO84b with other exocyst subunits by coimmunoprecipitation in transgenic *Arabidopsis* lines constitutively expressing EXO84b tagged on the C terminus with green fluorescent protein (GFP). After immunoprecipitation using the anti-GFP antibody, we detected SEC10, SEC15b, and EXO70A1 by matrix-assisted laser-desorption ionization (MALDI) time-of-flight mass spectrometry in bands excised from the polyacrylamide gel; these bands were not present in wild-type and free GFP controls (Figure 1B). In addition, EXO70A1 and another subunit, SEC6, were also identified in the coimmunoprecipitate using specific antibodies (Figure 1C).

We conclude that EXO84b interacts directly at least with EXO70A1 and SEC15b. The exocyst subunits SEC6 and SEC10 were coimmunoprecipitated as a part of a complex, possibly the entire exocyst complex.

Arabidopsis T-DNA Insertion Mutants in *EXO84b* Are Sterile Dwarfs with Cytokinetic Defects

We characterized two T-DNA insertion mutant alleles, *exo84b-1* and *exo84b-2* (Figures 2A and 2B). The self-crossed progeny of heterozygous plants segregated 24% (n = 401) and 21% (n = 355), respectively, of dwarf plants that were confirmed by PCR genotyping to be homozygous for their respective T-DNA insertions. No full-length *EXO84b* transcript was detected in either of the lines by RT-PCR (Figure 2C). The phenotypic defect of the *exo84b-2* homozygous plants was more severe than that of *exo84b-1* homozygotes; we speculated that the *exo84b-1* allele transcript could be spliced correctly at low frequency. However, we were unable to detect the full-length transcript even when the RT-PCR cycle number was increased to 35.

To confirm that the observed phenotypic defects are indeed caused by mutations in the *EXO84b* locus, we complemented both mutant alleles with the EXO84b protein fused to GFP. We used *35S-EXO84b-GFP* and *EXO84b-EXO84b-GFP* constructs to complement *exo84b-1* and *exo84b-2* lines, respectively. The complemented homozygous plants of both alleles exhibited wild-type appearance (Figure 2D). These results together with the finding that EXO84b-GFP coimmunoprecipitated the other exocyst subunits (see above) suggest that the C-terminal GFP

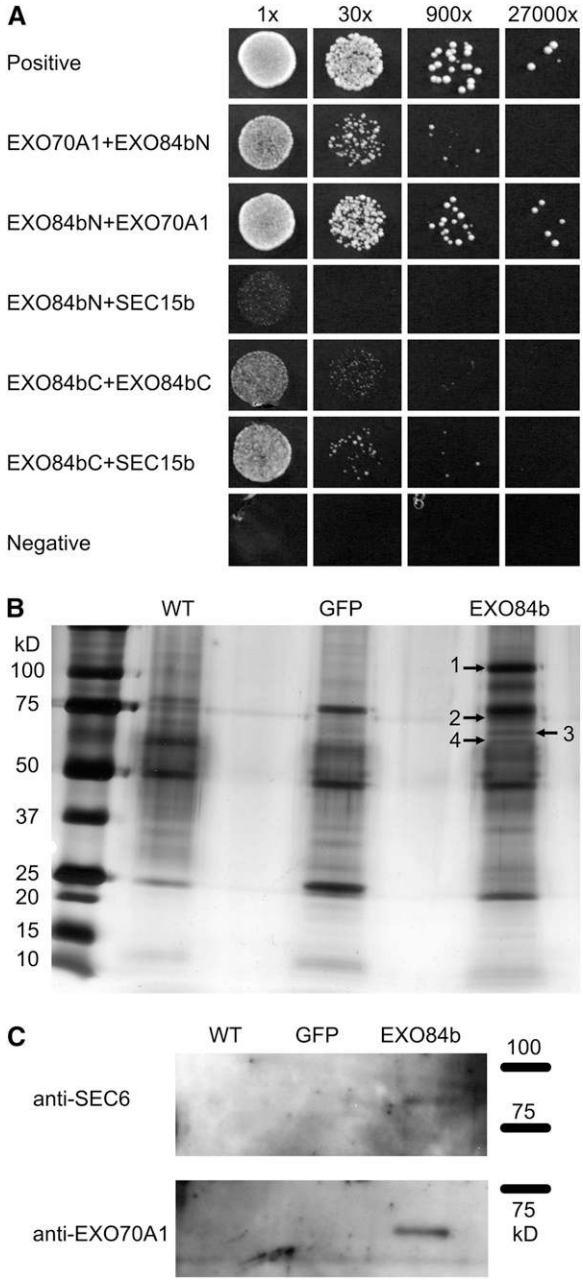

Figure 1. EXO84b Interacts with Other Exocyst Subunits.

(A) Pairwise interactions of EXO84b N- and C-terminal fragments in the yeast two-hybrid system with exocyst subunits EXO70A1 and SEC15b. The strength of interactions is demonstrated by a dilution series (indicated on the top). Binding and activation domains are denoted on the left and right, respectively.

(B) and **(C)** Coimmunoprecipitation of exocyst subunits with GFP-tagged EXO84b.

(B) EXO84b, SEC15b, SEC10, and EXO70A1 (1, 2, 3, and 4, respectively) were identified in the immunoprecipitate by mass spectrometry.

(C) SEC6 and EXO70A1 were detected by immunoblotting. Approximate protein molecular mass in kilodaltons is indicated, and the samples were loaded in the same ratio as in **(B)**.

tag does not interfere with EXO84b function, and the fusion protein is able to complement the *exo84b* phenotypic defects.

The uncomplemented *exo84b* homozygotes were sterile with extremely reduced stature. True leaves were angular, with small and irregularly developed trichomes or with trichome subsidiary cells without a trichome present (Figures 2E and 2F). The leaf surface of both *exo84b* lines showed defects in epidermal cell expansion, decreased jigsaw puzzle interlocking, and a high number of collapsed cells (Figures 3B and 3C).

On the cellular level, the leaf epidermis of both mutant lines contained cell wall stubs. There were two types of cell wall stubs: short stubs bulging from the periphery of the cell and long cell walls stubs spanning nearly the whole cell width. Occasionally, aberrant star-like cell plates stretched in the center of a cell were observed (Figures 3D to 3G). None of these deviations were observed in wild-type controls. When abaxial sides of true leaves of 15-d-old seedlings were examined, the cell wall stubs were detected in 3.5% of *exo84b-1* cells (1300 cells on four leaves analyzed) and 2% of *exo84b-2* cells (700 cells on four leaves).

Cytokinetic defects were obvious in stomata development. We documented that 12-d-old leaves of both *exo84b* mutants contained morphologically defective stomata (Figure 4A). Their defects ranged from aberrant highly asymmetric stomata and stomata with imperfectly divided guard cells with incomplete ventral walls to single guard cells lacking any viable counterparts (Figure 4B). By contrast, we never found such deviations in wild-type controls.

The *exo84b* Mutants Accumulate Vesicles

The exocyst has been shown to be involved in the post-Golgi secretion in fungi and animals. For example, Guo et al. (1999a) observed accumulation of secretory vesicles in yeast *exo84* mutants. We examined leaves of *Arabidopsis exo84b* mutants on the ultrastructural level using transmission electron microscopy.

We focused on cells in the epidermis that were not fully vacuolated and contained dense cytoplasm. Focusing on this cell type allowed an easy comparison of similar developmental stages between wild-type and mutant leaf cells. In the *exo84b-1* and *exo84b-2* mutant cells, vesicles were dramatically accumulated in 16 of 45 cells examined (Figure 5B) and often contained fibrous electron-dense material. In the wild-type cells, similar vesicle accumulation was not observed (Figure 5A). Instead, vesicles were scattered around the Golgi apparatus.

The epidermis of mutant leaves also contained electron dense, presumably aborted, cells that were stuffed with vesicles (Figure 5C). These cells most likely correspond to the dead cells described above. However, leaves of *exo84b* mutants also possess cells morphologically similar to wild-type cells, pointing to a large spectrum of phenotypes observed in mutant leaves (Figures 3 and 4).

EXO84b-GFP Localizes at the Early and Postcytokinetic Cell Plate

To examine the EXO84b subcellular localization, we used *EXO84b-GFP* stably transformed *Arabidopsis* plants, in which the expression was driven by the constitutive *35S* promoter or by

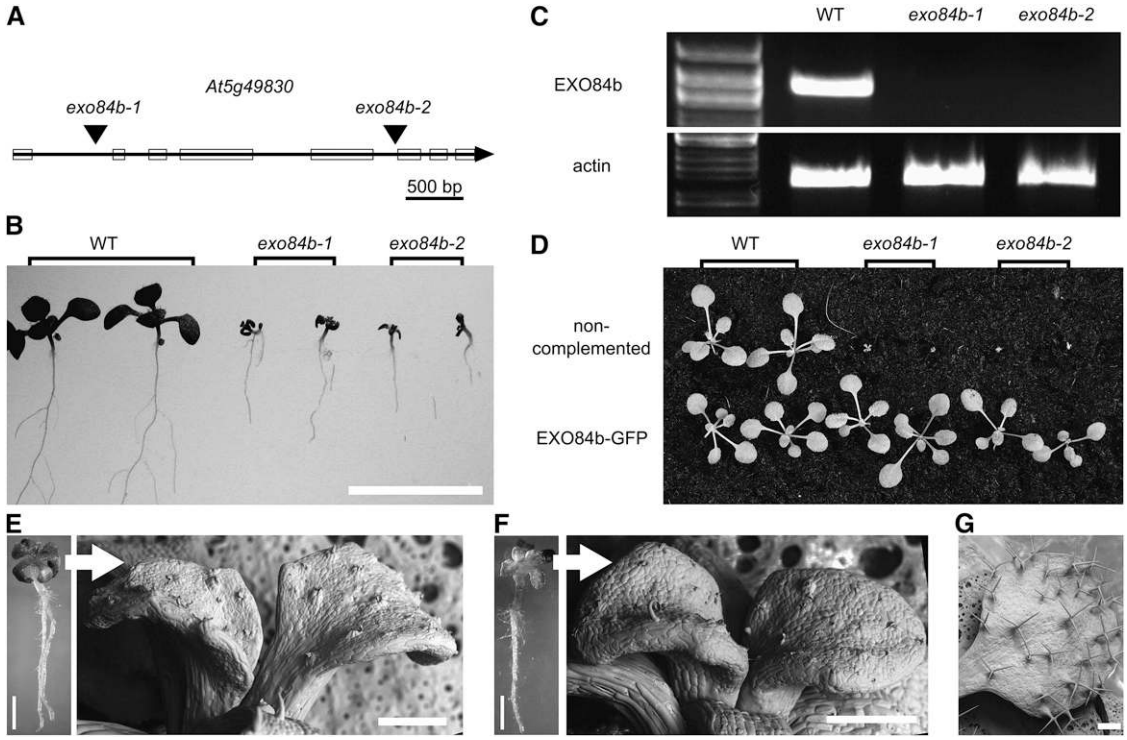

Figure 2. Mutations in *EXO84b* Lead to a Severe Growth Phenotype.

(A) *EXO84b* gene structure with T-DNA insertion positions indicated.
(B) Wild-type, *exo84b-1*, and *exo84b-2* seedlings 10 d after germination. Bar = 1 cm.
(C) RT-PCR of the full-length *EXO84b*. The *ACTIN7* control was amplified from the same cDNA.
(D) Comparison of uncomplemented (top row) and *exo84b-1* and *exo84b-2* plants complemented by EXO84b-GFP expressed under 35S and EXO84b promoter (bottom row), respectively.
(E) to **(G)** *exo84b-1* **(E)** and *exo84b-2* **(F)** mutants have minute true leaves with defective trichomes. On the left, 10-d-old seedlings (bar = 1 mm); on the right, detail of the true leaves is shown (environmental scanning electron microscopy). Wild-type leaf is shown in **(G)**. Bars = 200 μm.

the native *EXO84b* promoter. EXO84b-GFP expressed under the control of either promoter decorated plasma membranes weakly and strongly labeled postcytokinetic walls plasma membrane in leaf and root cells (Figures 6A to 6D). In the case of the *35S* promoter, we observed bright cortical particles of unknown identity (visible in Figure 6B), probably caused by the constitutive promoter overexpression.

To get deeper insight into the EXO84b-GFP cytokinetic localization, we aimed our attention at the root meristem of 4- to 7-d-old *Arabidopsis* seedlings as this tissue is easily accessible to live-cell imaging and harbors frequent and predictably localized dividing cells. Moreover, Seguí-Simarro et al. (2004) reported no differences between cell plate formation in root and shoot meristematic cells. The *35S*-driven EXO84b-GFP signal was stronger than that of the native promoter, but the dynamics and localization of both was similar. During cytokinesis, the EXO84b-GFP signal was associated with the newly emerged cell plate and weakly with the growing cell plate. It started to substantially accumulate at the cell plate insertion site after the cell plate attached to the mother wall (Figure 6E). The precise timing of EXO84b-GFP accumulation at the postcytokinetic wall was dependent on the mode of cell plate growth. In symmetrically growing cell plates (where the entire cell plate edge fuses with the mother membrane simultaneously), the signal appeared at the moment of cell plate insertion or shortly after. In cell plates that were expanding asymmetrically, and so their edge reached one side of the cell sooner than the other, the EXO84b-GFP signal usually localized at the insertion site only after fusion of both cell plate edges with the membrane. Subsequently, the signal spread into the entire cell plate (Figure 6E). The postcytokinetic wall signal was not homogeneous; it showed fluctuating maxima (Figure 6C). After completion of cytokinesis, EXO84b-GFP remained associated with the postcytokinetic wall, with its intensity decreasing to the level of the surrounding cells in approximately one hour after its appearance.

SEC6, SEC8, SEC15b, and EXO70A1 Exocyst Subunits Share the Cytokinetic Localization with EXO84b

To learn whether the observed cytokinetic localization pattern is unique to EXO84b, or is rather a feature of the exocyst complex, we analyzed localizations of several other exocyst subunits during cytokinesis. We prepared *Arabidopsis* lines expressing GFP-tagged versions of SEC6, SEC8, SEC15b, and EXO70A1.

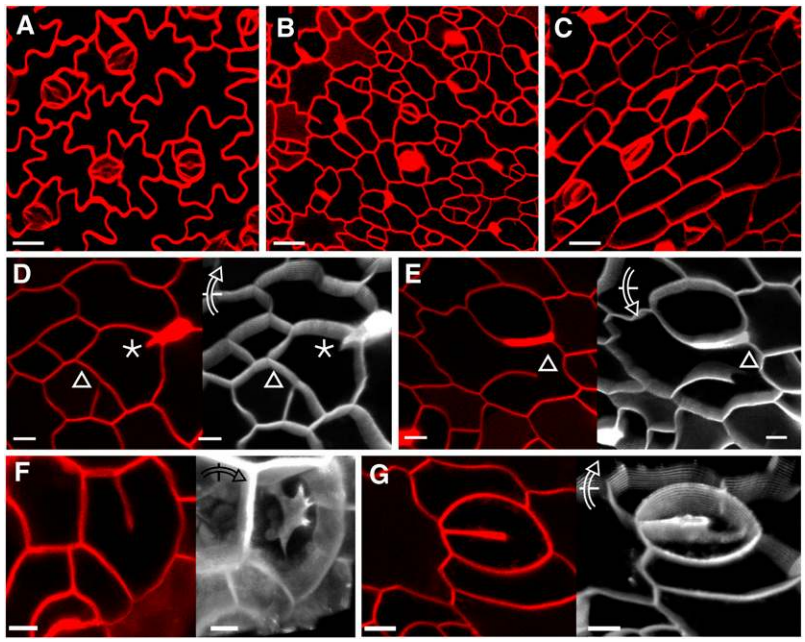

Figure 3. *exo84b* Mutants Have Cell Wall Stubs.

(A) to **(C)** FM4-64–stained abaxial 3rd leaf epidermis of wild-type **(A)**, *exo84b-1* **(B)**, and *exo84b-2* **(C)** seedlings.
(D) to **(G)** FM4-64–stained abaxial leaf epidermal cells of *exo84b-1* mutant plants. A single confocal section is shown in red (left) with corresponding three-dimensional reconstruction from serial confocal sections shown in white with the rotation indicated (arrow). Epidermal cells contained short cell wall stubs (asterisk) **(D)**, long unfinished cell walls (triangle) (**[D]** and **[E]**), and aberrant cell plates **(F)**.
(G) Imperfectly separated guard cells with a developed stomatal pore. After the three-dimensional reconstruction, unfinished cell plate connected with the stomatal pore is evident. Bars = 10 μm.

All of them showed cytoplasmic localization, weak plasma membrane labeling, and strong association with postcytokinetic walls (Figures 7 and 8).

During the onset of cytokinesis, SEC6-GFP, GFP-SEC8, GFP-SEC15b, and EXO70A1-GFP strongly associated with the cell plate at the moment of its emergence, appearing as a localized flash of fluorescence lasting 30 to 60 s. During cell plate growth, the signal decreased, until reappearance at the time of cell plate insertion (Figures 7 and 8).

SEC6-GFP and GFP-SEC8 were expressed under control of their native promoters, and GFP-SEC15b and EXO70A1-GFP expression was driven by the *35S* promoter. Importantly, both types of expression yield identical localization and dynamics in cytokinesis.

Taken together, these results reinforce our previous data suggesting that the plant exocyst acts as a complex (Hála et al., 2008) and further argues that the exocyst complex, and not solely EXO84b, functions in cytokinesis.

The *exo70A1* Mutant Is Defective in the Cell Plate Assembly Phase

As the cytokinetic localization is shared among all exocyst subunits tested, we asked whether cytokinesis is compromised in other exocyst mutants as well. Another viable available *Arabidopsis* exocyst mutant is *exo70A1* (described in Synek et al., 2006), which has a less severe phenotypic defect than *exo84b* mutants, and does not exhibit the cytokinetic defects described in the case of *exo84b* mutants.

We analyzed cytokinesis in root tips of 4-d-old *exo70A1* mutants and wild-type plants. Root length of *exo70A1* mutants was reduced by 22% (*exo70A1*, 11.7 ± 1.6 mm, n = 20; wild-type, 15.0 ± 1.8 mm, n = 41; ± indicates SD). To investigate whether the delay in cytokinesis might contribute to this difference, we measured the time needed for cytokinesis completion. We labeled cell plates with FM4-64 and determined the time from cell plate appearance to cell plate straightening between the mother walls. We normalized time to the cell plate area (estimated as a circle with diameter of the finished cell plate) obtaining a cell plate expansion rate. However, there was no significant difference between *exo70A1* mutant plants (0.17 ± 0.05 $\mu m^2\ s^{-1}$, n = 32) and wild-type controls (0.19 ± 0.10 $\mu m^2\ s^{-1}$, n = 19; Figure 9A).

We further focused on the cell plate morphology, especially around the moment of its appearance. We used three-dimensional reconstruction of time-lapsed series of confocal sections. In wild-type root meristem cells, the cell plate emerged in the middle of the cell, typically as a filled circle or as a few small patches, which quickly fused and gave rise to the cell plate. The cell plate arose from vesicles invisible in the confocal microscope (Figure 9C). However, in the *exo70A1* mutants, the cell plate emerged by fusion of visible spots, forming a donut-shaped or

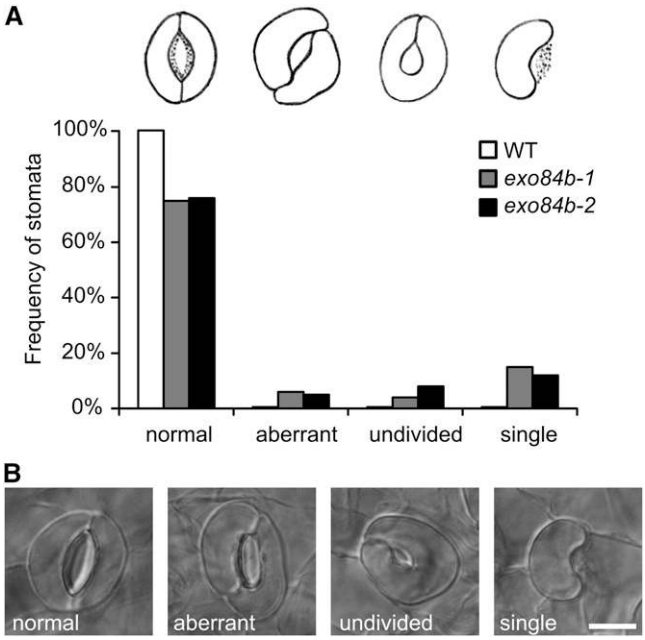

Figure 4. Stomata Morphology in *exo84b* Mutants.

(A) Frequency of stomata sorted by their morphology in leaves of 12-d-old wild type (white), *exo84b-1* (gray), and *exo84b-2* (black); $n > 200$ for each genotype. The category "normal" also includes developing stomata.

(B) Most abundant stomata types: normal stomata, aberrant stomata with highly asymmetric guard cells, stomata with incompletely divided guard cells, and stomata consisting of a single guard cell. Bar = 10 μm.

horseshoe-shaped structure with an empty space in its center (Figure 9C). Mutant cell plates further expanded not only centrifugally but also centripetally to fill the central gap. Thus, it was difficult to distinguish mutant and wild-type cell plates in the late phase of their expansion (Figure 9D). We classified the cell plate shape into three categories, solid, patchy, and donut/horseshoe-shaped, and found that the dominant type in *exo70A1* mutants was the donut/horseshoe, which was never observed in the wild type (Figure 9B). Unfortunately, we were unable to perform a similar analysis with the *exo84b* mutants due to their slow growth and infrequent cell divisions. However, the few *exo84b-1* cell plates we observed generally resembled that of the wild type.

These results suggest that EXO70A1 is important in the initial cell plate assembly phases, whereas the later centrifugal cell plate growth is likely unaffected by EXO70A1 deficiency.

DISCUSSION

The *Arabidopsis* Exocyst Includes the EXO84 Subunit

We showed previously that the plant exocyst complex consists of SEC3, SEC5, SEC6, SEC10, SEC15, and EXO70 subunits (Hála et al., 2008). Here, we show that EXO84 as well is a part of the *Arabidopsis* exocyst complex. This is of interest, as genomes of *Excavata* and *Chromalveolata* encode incomplete sets of exocyst proteins, with the EXO84 subunit commonly lost (Koumandou et al., 2007). In human cells, the Exo84 protein was suggested to bridge exocyst subcomplexes composed of Sec10/Sec15/Exo84 and Sec5/Sec6/Sec8/Exo70 (Moskalenko et al., 2003). In yeast, Sec10, Sec15, and Exo70 subunits require functional Exo84 for their localization to the bud tip (Zhang et al., 2005b). Another role for yeast Exo84 is implied by direct interaction with t-SNARE regulators Sro7 and Sro77. This interaction is mediated by the N terminus of Exo84, whereas the C terminus

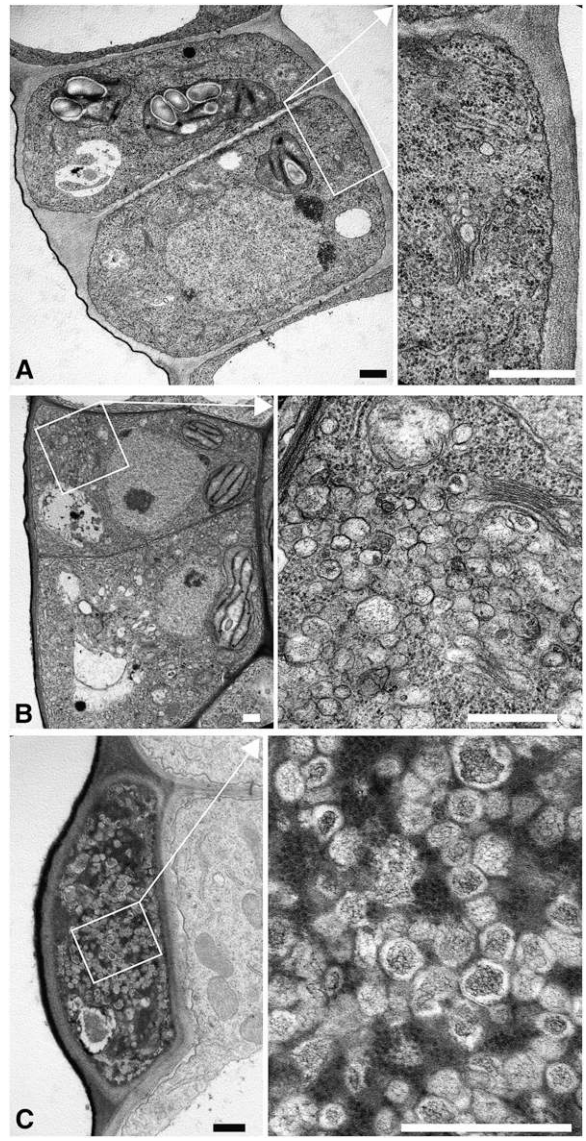

Figure 5. *exo84b* Mutants Accumulate Vesicles.

Transmission electron microscopy sections of epidermal cells of the wild type **(A)** and *exo84b* mutants (**[B]** and **[C]**). A proportion of *exo84b* mutant cells accumulated vesicles **(B)**. A dead cell loaded with vesicles in the epidermis of *exo84b*-2 mutant plant **(C)**. The boxed areas are shown in higher magnification on the right, with the positions of the boxes indicated with arrows. Bars = 0.5 μm.

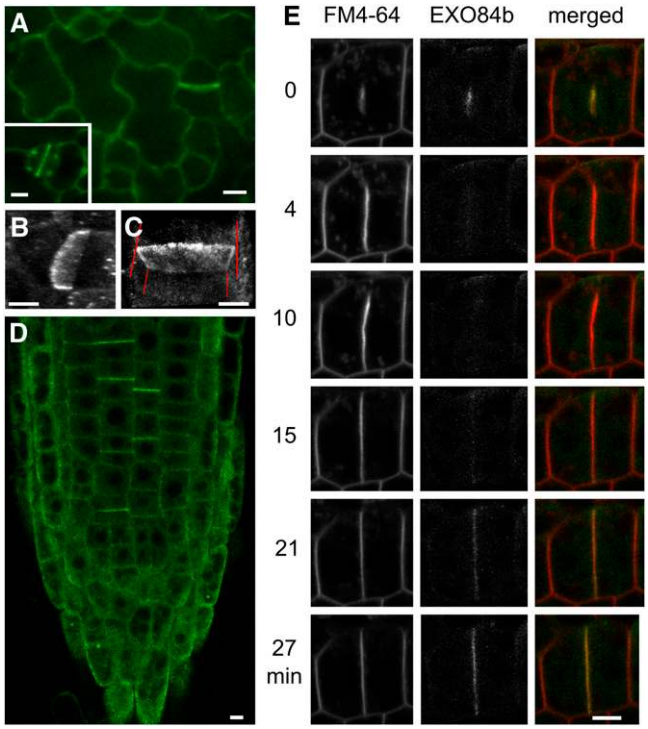

Figure 6. EXO84b-GFP Fusion Protein Localizes to the Cell Plate and Postcytokinetic Wall.

(A) Abaxial epidermis of a developing leaf shows strong EXO84b-GFP signal at the cross walls. Recently divided guard cells with EXO84b-GFP–labeled ventral walls are shown in the inset.
(B) and **(C)** Three-dimensional reconstructions of CLSM sections of the leaf **(B)** and root **(C)** cross walls. In **(B)**, the 35S-EXO84b-GFP particles are visible. In **(C)**, perpendicular cell walls in respect to the newly formed cell walls are indicated with red lines.
(D) EXO84b-GFP labels postcytokinetic walls in the *Arabidopsis* root.
(E) Time series of a root growing cell plate stained with FM4-64. EXO84b-GFP signal localized to the newly emerged cell plate. In the cell plate growth phase, the signal intensity decreases and reappears with the cell plate insertion into the mother plasma membrane. In **(A)**, **(D)**, and **(E)**, EXO84b was expressed under *EXO84b* promoter and in **(B)** and **(C)**, under *35S* promoter. In the confocal laser scanning microscopy sections, bars = 5 μm.

appears to be responsible for binding other exocyst subunits (Zhang et al., 2005a). The *Arabidopsis* EXO84b is distinct from the yeast homolog because both its termini interacted with other exocyst subunits; SEC15b and EXO70A1. Interestingly, intra-exocyst interactions differ among yeast, animals, and plants as detected by the yeast two-hybrid assay. Exo84 interacts with Sec5 and Sec10 in yeast, whereas with Sec5, Sec15, and Exo70 in animals (reviewed in Munson and Novick, 2006), indicating higher conservation of interactions between animals and plants.

We characterized two T-DNA insertion mutants in the *EXO84b* gene. The C-terminally located insertion exerted more severe phenotypic deviation than the N-terminally located one. It is possible that in the N-terminal insertion, EXO84b transcripts are correctly spliced at a very low frequency, which is under the detection limit of RT-PCR. Both lines had similar phenotypic defects that could be complemented by expression of GFP-tagged EXO84b.

Mutations in *EXO84b* lead to severe growth retardation and sterility. Mutant epidermal cells displayed cell wall stubs, indicating a failure in cytokinesis. The guard cell cytokinesis and morphogenesis were adversely affected. In this respect, the *exo84b* phenotype resembles that of other stomatal cytokinesis mutants: *scd1* and *cyd1* (Yang et al., 1999; Falbel et al., 2003). It is noteworthy that SCD1 is also involved in vesicle trafficking. On the subcellular level, a portion of mutant cells accumulated a high concentration of vesicles, consistent with the idea of exocyst function as a secretory vesicle tethering complex. This is reminiscent of the ultrastructural defect of vesicle accumulation in the first yeast exocyst mutants identified in the original secretory screen (Novick et al., 1980) and later found also in yeast *exo84* mutants (Guo et al., 1999a). Vesicles accumulated in the *exo84b* mutant are mostly filled with fibrous contents, suggesting possible pectin and xyloglucan nature of the cargo.

In the sporophyte, the phenotypic defect of *exo84b* mutants is more severe than that of other viable plant exocyst mutants described to date (Zm *rth1*, Wen et al., 2005; At *exo70A1*, Synek et al., 2006; At *sec5a* and At *sec8-4*, Hála et al., 2008). One possible explanation is that EXO84b is particularly important for exocyst assembly and/or stability. Alternatively, the other known mutations might only incompletely eliminate the function of the affected subunit due to genetic and functional redundancy among paralogous genes (in case of EXO70, SEC5, and RTH1; maize homologs of SEC3) or only partial elimination of the function (in case of weak *sec8* mutations; Cole et al., 2005).

The Exocyst Is Involved in Cell Plate Initiation

Several pioneering electron tomography studies have provided a model of membrane remodeling during cytokinesis (Samuels et al., 1995; Otegui and Staehelin, 2004; Seguí-Simarro et al., 2004). In early cytokinesis, vesicles arrive at the equatorial plane into the cell plate assembly matrix (a cocoon-like, ribosome-excluding domain around the forming cell plate) to form a late anaphase vesicle cloud. Their fusion might be initiated by abundant exocyst-like tethering complexes. Fused vesicles are stretched into dumbbells, fuse with other vesicles, and further join together giving rise to a tubulo-vesicular network. The network ultimately forms a fenestrated sheet that is consolidated with callose. Whereas the involvement of several SNARE-type proteins in cell plate vesicle fusion was documented (Lauber et al., 1997; Heese et al., 2001), the identity of tethering exocyst-like complexes observed by electron tomography has not been resolved (Otegui et al., 2005).

In dividing *Arabidopsis* root cells, we observed that exocyst subunits associated strongly with the initiating cell plate, corresponding to the late anaphase vesicle cloud and tubulo-vesicular network stages of its development. The importance of the exocyst for the cell plate initiation is supported by the defect we described in early cytokinesis of the *exo70A1* mutant where the initial cell plate morphology is compromised. The center of mutant cell plates showed a gap in the membrane signal. The gap was filled centripetally during subsequent cell plate growth.

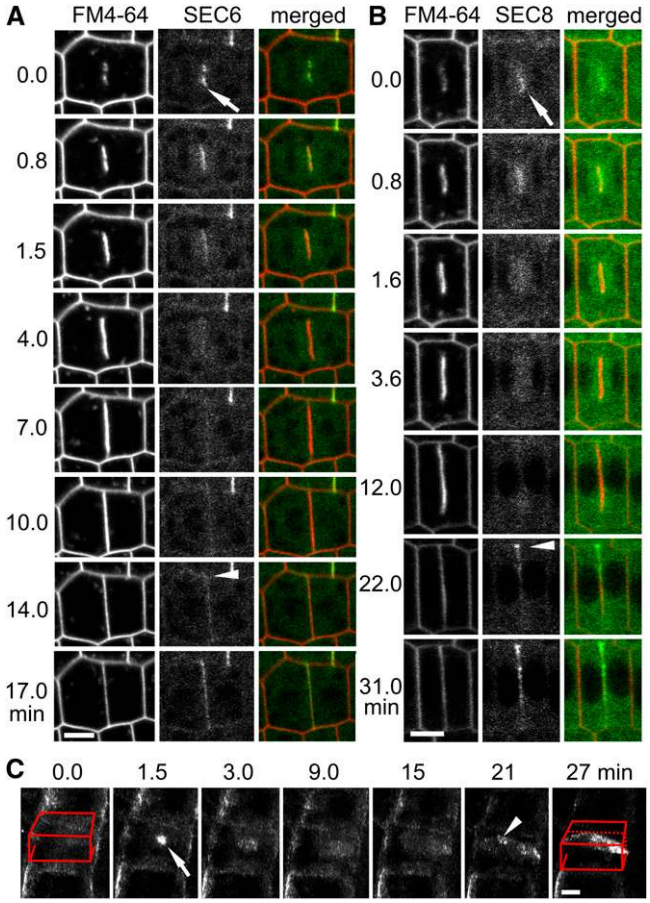

Figure 7. SEC6 and SEC8 Localize to the Cell Plate and Postcytokinetic Wall.

(A) and **(B)** Time series showing SEC6-GFP **(A)** and GFP-SEC8 **(B)** localization during cytokinesis of root meristem cells stained with FM4-64. Arrow denotes strong association of both proteins with the new cell plate. Arrowhead points to cell plate insertion site labeled by SEC6-GFP and GFP-SEC8. Single confocal laser scanning microscopy sections.
(C) The initial flash of SEC6-GFP signal (see text) is marked with an arrow. Arrowhead points to SEC6-GFP postcytokinetic wall signal. The position of the cell is indicated with red lines, three-dimensional reconstruction of CLSM sections taken in a time series, slanted backwards. Bars = 5 μm.

We assume that the gap is caused by the inability of vesicles to fuse efficiently; however, disturbed vesicle trafficking to the phragmoplast center cannot be excluded. In yeast and mammalian cells, EXO70 localizes to the cleavage furrow and midbody in dividing cells, and depletion of EXO70 results in cytokinesis collapse and mislocalization of secretory vesicles transport regulators RAB11 and FIP3/4 (Fielding et al., 2005).

Subsequently, the fluorescence of GFP-labeled exocyst components was substantially weaker in the growing cell plate. These results distinguish the initial cell plate assembly phase from later peripheral cell plate growth. If the exocyst was involved in the peripheral cell plate growth, one would expect the exocyst to form a ring on the margin of the growing plate, similar to Rab GTPases from the Rab-A2 family (Chow et al., 2008). Such a ring was not observed; instead, the exocyst subunits only weakly labeled the whole growing cell plate.

Although the canonical role of the exocyst inheres in secretory vesicle tethering to the plasma membrane (TerBush et al., 1996), our data strongly implicate an additional plant-specific role of the exocyst in the initial cell plate assembly phase, where the vesicles fuse to each other or to the cell plate precursors.

The Exocyst Plays Roles in the Final Stages of Cytokinesis

Once the growing cell plate approaches the plasma membrane, hundreds of finger-like projections emanate from the cell plate margin and fuse with the plasma membrane (Samuels et al., 1995). The fusion site is marked by the TANGLED protein (Walker et al., 2007). The T-PLATE protein has been proposed to act in cell plate insertion (Van Damme et al., 2006). It contains domains similar to the β-COP proteins and adaptins involved in vesicle formation, is present in the growing cell plate, and is most strongly localized around the area of cell plate insertion site. Judging from the observed unattached cell plates observed in the *exo84b* mutants and exocyst subunit localization in late cytokinesis, we assume that the exocyst participates also in the cell plate to plasma membrane fusion.

With the cell plate insertion, secondary cell plate assembly matrices arise in the cell plate to close the remaining fenestrae present (Seguí-Simarro et al., 2004). After the insertion, GFP-labeled exocyst subunits strongly localized to the postcytokinetic wall, where they remained localized throughout the cell plate maturation. These observations suggest that the *Arabidopsis* exocyst complex may be involved in the closing of fenestrae remaining in the immature wall. Similarly to its early

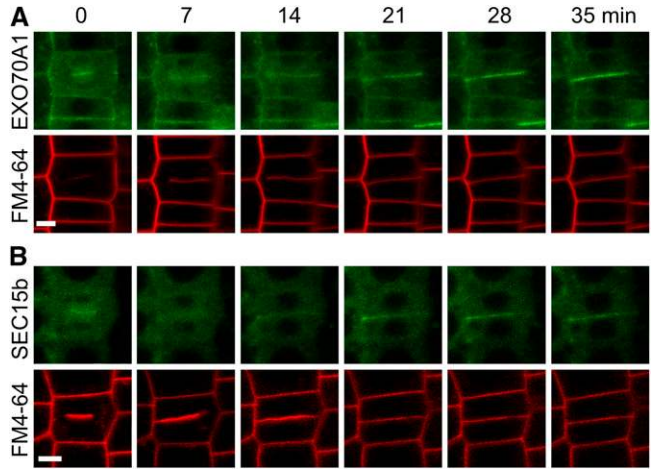

Figure 8. Localization Dynamics of GFP-EXO70A1 and GFP-SEC15b during Cytokinesis.

GFP-EXO70A1 and GFP-SEC15b localize to the nascent cell plate; later, the signal reappears at the time of cell plate insertion to the mother wall and expands along the whole area of the postcytokinetic wall. Cell membranes were stained by FM4-64. Single confocal laser scanning microscopy sections are displayed. Bars = 5 μm.

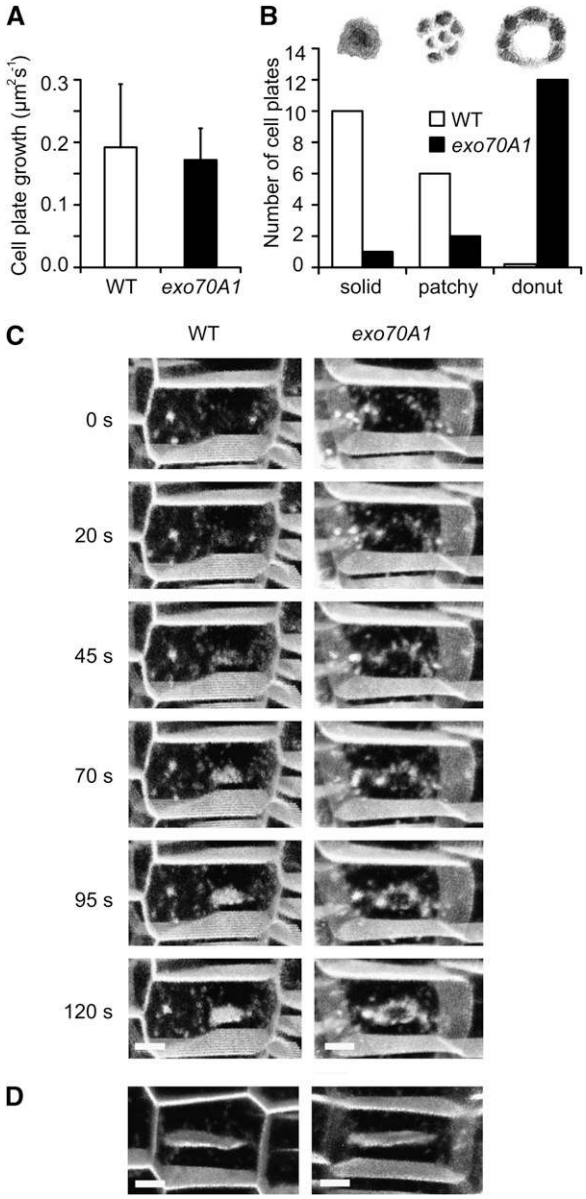

Figure 9. Analysis of *exo70A1* Mutant Cytokinesis.

(A) Mean cell plate growth rate of the wild type and *exo70A1*; error bars represent SD.

(B) Classification and count of solid, patchy, and donut-shaped cell plate types as sketched at the top found in wild-type and *exo70A1* mutant cells.

(C) Initial phases of cytokinesis of the wild type (left) and *exo70A1* (right) in cells stained with FM4-64; donut-shaped cell plate is obvious in the mutant.

(D) In later phases, the wild-type and *exo70A1* cell plates were not distinguishable. Bars = 5 μm.

cytokinesis role, the exocyst could trigger vesicle fusion in the associated secondary cell plate assembly matrices. The cytokinetic defects in *exo84b* mutants could result from difficulties with closing the fenestrae in the planar sheet stage. The presumably unstable planar fenestrated sheet cell plates might collapse and result in cell wall stubs and defective stomata with incomplete ventral walls observed.

The postcytokinetic wall maturation and cell plate straightening is triggered by the cell plate contact with the mother wall (Mineyuki and Gunning, 1990). Maturation leads to complex changes in the cell wall structure and composition involving callose exchange for cellulose, redistribution of cell wall material, and secretion of cell wall modifying proteins (Samuels et al., 1995; Matar and Catesson, 1988; Hall and Cannon, 2002). The exocyst could act in trafficking of vesicles containing cell wall components and cellulose synthase complexes, which are assembled in the Golgi apparatus and then deposited to the plasma membrane (Crowell et al., 2009; Gutierrez et al., 2009). This is consistent with the exocyst role in pectin delivery during seed coat development in *Arabidopsis* (Kulich et al., 2010). Maturation involves connecting the cell plate lumen with the apoplast after the cell plate insertion (Cutler and Ehrhardt, 2002) and modifying the cell wall at the insertion site. The RSH extensin is accumulated in the cell wall at this site (Hall and Cannon, 2002). It is possible that the exocyst could act in the delivery of extensin and similar proteins to the insertion site. Interestingly, in *S. pombe*, the exocyst is necessary for hydrolytic enzyme delivery necessary for cell separation (Martín-Cuadrado et al., 2005). The exocyst and associated hydrolytic enzymes localize to a cortical ring that surrounds the septum. Remarkably, the exocyst localizes to a peripheral ring in the midbody in mammalian cells and probably act in the fusion of vesicles with the plasma membrane (Gromley et al., 2005).

There have been a few proteins reported to act in cell plate maturation with localization similar to the postcytokinetic localization of the exocyst proteins. AIR9 is associated with cortical microtubules in interphase cells (Buschmann et al., 2006). During cytokinesis, it is recruited to the phragmoplast, and at the moment of cell plate insertion, it relocates to the insertion site and later appears more centrally in the cell plate. Another postcytokinetic cross wall–localized protein is a class VIII myosin for which a role in cell plate maturation was suggested (Reichelt et al., 1999).

Based on the cytokinetic defects in *Arabidopsis* exocyst mutants and on exocyst subunit localizations, we argue that the exocyst is involved in cytokinesis in the plant cell. We demonstrated that the exocyst likely is associated with and

Table 1. Accession Numbers and T-DNA Insertion Lines Used in This Study

Gene	Accession Number	T-DNA Insertion Line
EXO84a	At1g10385	
EXO84b	At5g49830	GABI_459C01
EXO84b	At5g49830	SAIL_736_A04
EXO84c	At1G10180	
SEC6	At1g71820	
SEC8	At3g10380	SALK_057409
SEC10	At5g12370	
SEC15b	At4g02350	
EXO70A1	At5g03540	SALK_135462
ACTIN7	At5g09810	

may trigger the initial cell plate vesicle fusion. The exocyst subunits reside associated with the postcytokinetic wall where they might act in completing the fenestrated cell plate and in delivery of specific cargoes necessary for cell wall maturation. The exocyst localization at the cell plate insertion site in *Arabidopsis* resembles the ring localization of the exocyst during cytokinesis in *S. pombe* and the mammalian exocyst localization in the midbody (Gromley et al., 2005; Martín-Cuadrado et al., 2005). The role of the exocyst in late cytokinesis might be conserved between Opisthokonts and plants and therefore may be ancestral. Cutler and Ehrhardt (2002) suggested that there are two distinct phases of cell plate development: before and after the contact with the cell cortex. This concept is strengthened by the behavior of the exocyst subunits. In the future, it will be important to analyze in detail the molecular machinery controlling the exocyst action in cytokinesis and its possible functional connection to later stages of vesicle fusion mediated by SNARE complexes. The involvement of exocyst complex in plant cytokinesis regulation adds an important piece of evidence to support the idea of similarity of late cytokinesis mediated by midbody in animals and phragmoplast in plants.

METHODS

Yeast Two-Hybrid System

The yeast two-hybrid was performed as described previously (Hála et al., 2008): we used the Matchmaker GAL4 Two-Hybrid System 3 (Clontech), and all procedures followed the manufacturer's instructions. To test interactions between EXO84b and other exocyst subunits, we used constructs prepared by Hála et al. (2008). The EXO84b construct was divided into two fragments. EXO84bN (1 to 113 amino acids) and EXO84bC (373 to 752 amino acids) were subcloned into *pGADT7* and *pGBKT7*. As a positive control, murine p53 and SV40 large T-antigen proteins provided with the Matchmaker system were used, and as negative control, empty vectors were used. The dilution series was prepared as follows: A single colony was resuspended in sterile water and diluted in sterile water, and 10 μL was dropped onto -Ade-His-Leu-Trp plates and cultivated at 28°C.

Coimmunoprecipitation

Protein complexes with EXO84b-GFP fusion protein were isolated using the μMACS GFP tagged protein isolation kit (Miltenyi Biotec); the manufacturer's instructions were followed with following modifications: ~1.2 g of 10-d-old *Arabidopsis thaliana* seedlings were pulverized in liquid nitrogen, resuspended in 2 mL provided lysis buffer, and centrifuged 10,000*g* for 10 min at 4°C. The supernatants were equilibrated to the same protein concentration using the Bradford assay (Sigma-Aldrich). One hundred microliter of anti-GFP microbeads were added and incubated for 30 min on ice with shaking. The lysis buffer was used to wash the samples on the column, and immunoprecipitates were eluted with 70 μL of the elution buffer. Forty microliters were run on a gradient SDS-PAGE (6 to 20%; prepared as described in Smith and Bell, 1986), and the rest was used for immunoblotting.

Protein Gel Blot and Mass Spectrometry Analysis

Proteins were blotted onto a nitrocellulose membrane and blocked overnight at 4°C with 5% nonfat dry milk in PBS (137 mM NaCl, 2.7 mM KCl, 10 mM Na_2HPO_4, and 2 mM KH_2PO_4, pH 7.4) supplemented with 0.1% Tween 20. Primary antibodies anti SEC6 and anti-EXO70A1 (Hála et al., 2008) were diluted 1:1000 and incubated with the membranes for 2 h at room temperature in the blocking solution. Horseradish peroxidase–conjugated antibody (Promega) was applied followed by chemiluminescent ECL detection (Amersham).

The gels were stained with ProteoSilver Plus Silver Stain Kit (Sigma-Aldrich). Individual bands were placed in microtubes and destained with destaining solutions supplied with the kit, washed five times with water, and dehydrated with acetonitrile (ACN) prior to trypsin digestion. ACN was discarded and microtubes with samples were left open to allow the ACN to evaporate. Five nanograms of trypsin (Promega) in 10 μL of 50 mM ABC were added to the gel. Samples were incubated at 37°C overnight. Trifluoroacetic acid and ACN were added to reach final concentrations of 1% trifluoroacetic acid and 30% ACN. Samples were sonicated for 10 min, and the supernatant was mixed 1:1 with water in a HPLC vial.

Liquid chromatography-MALDI analyses were performed using Ultimate 3000 HPLC system (Dionex) coupled to Probot microfraction collector (Dionex). Tryptic peptides were loaded onto a PepMap 100 C18 RP column (3-μm particle size, 15 cm long, 75-μm internal diameter; Dionex) and separated by a gradient of 5% (v/v) ACN, 0.1% (v/v) trifluoroacetic acid to 80% (v/v) ACN, 0.1% (v/v) trifluoroacetic acid over a period of 60 min. The flow rate was set to 300 nL/min. Eluate was mixed 1:3 with matrix solution (2 mg/mL α-cyano-4-hydroxycinnamic acid in 80% ACN) prior to spotting onto a MALDI target. Spectra were acquired on a tandem time-of-flight analyzer (Applied Biosystems/MDS Sciex) equipped with an Nd:YAG laser (355 nm, firing rate of 200 Hz).

Peak lists from the mass spectrometry spectra were generated by 4000 Series Explorer V 3.5.3 (Applied Biosystems/MDS Sciex) without smoothing, and peaks with local signal-to-noise ratio >5 were picked and searched by local Mascot v.2.1 (Matrix Science) against the National Center for Biotechnology Information nonredundant database (June 24, 2009; 9,144,919 sequences). Database search criteria were as follows: enzyme, trypsin, one missed cleavage allowed; taxonomy, *Arabidopsis* (60,098 sequences); fixed modification, carbamidomethylation; variable modification, Met oxidation; peptide mass tolerance, 80 ppm; tandem mass spectrometry fragment tolerance 0.2 D.

T-DNA Insertion Mutant Analysis and RT-PCR

The T-DNA insertion lines were Columbia-0 ecotype of *Arabidopsis*. Both lines were backcrossed two times into the Columbia-0 background. The *exo84b-1* line was obtained from GABI-Kat (Rosso et al., 2003). Our preliminary observations suggested mistakenly that the *exo84b-1* allele caused a male-specific transmission defect (Hála et al., 2008). This was due to overlooking homozygous seedlings that visually resembled the sensitive plants on sulfadiazine selection (T-DNA insertion). The *exo84b-2* line was part of the SAIL collection (Sessions et al., 2002) distributed by Nottingham Arabidopsis Stock Centre (www.Arabidopsis.info). The primers used for genotyping this line were RP, 5′-TGTAGATGTGCTGGTAAGAGC-3′; LP, 5′-GGACCTTCCTCAATGTCATCC-3′; and the LB3 primer, 5′-CATCTGAATTTCATAACCAATCTCG-3′. The location of both T-DNA insertions within the *EXO84b* gene was verified by sequencing from each end of the insert. To test the presence of the full-length gene product, total RNA was isolated using the RNeasy kit (Qiagen), and the cDNA was synthesized using the Transcriptor High Fidelity cDNA synthesis kit (Roche). PCR was performed using the following primer pair: 5′-TTGGATCCGTTTAACGATGGCGGCGAAGA-3′ and 5′-TGAGCTCTCAATAGCTGCCATGAGATCT-3′. As a control, the *ACTIN7* gene was amplified using these primers: 5′-GAAACTCACCACCACGAACCA-3′ and 5′-GCCGATGGTGAGGATATTCAGC-3′.

Arabidopsis seeds were planted into Jiffy pellets (www.jiffypot.com) or surface sterilized, stratified at 4°C for 3 to 5 d, and planted on vertical agar plates (half-strength Murashige and Skoog, 1% [w/v] sucrose, 1.6% agar,

and vitamins or half-strength Murashige and Skoog with 2% sucrose in the case of the GFP-SEC8 line). Plants were grown in a climate chamber at 22°C under long-day conditions (16 h of light per day).

Cell wall stubs were counted on abaxial side of 10- to 13-d-old true leaves stained with 10 μM FM4-64 using the ImageJ program (Abramoff et al., 2004). For stomata analysis, the 11-d-old seedlings were fixed in 3:1 ethanol:acetic acid overnight, washed with 70% ethanol and water, incubated for 1 h in 1% SDS + 200 mM NaOH, washed again with water, and observed with an Olympus BX51 microscope.

Fluorescent Protein Construction and Transformation

Construct of *EXO84b* used in Hála et al. (2008) was transferred into binary vector *pK7FWG2* (Karimi et al., 2002) using the Gateway system (Invitrogen). A region of 460 bp upstream the *EXO84b* start ATG were cloned into the *pENTR1A* vector containing the *EXO84b* and further transferred into *pGWB4* (Nakagawa et al., 2007). *SEC6* was cloned into *pENTRY* vector and transferred into *pK7FWG2*. Using *Sac*I and *Eco*RI, the *35S* promoter was excised and replaced by a 1000-bp presumptive *SEC6* promoter region, previously cloned into *pDRIVE* vector (Qiagen PCR cloning kit), and cut out as an *Eco*RI and *Bam*HI fragment. Cohesive *Eco*RI end ligation with linearized *pK7FWG2-SEC6* was performed, followed by blunting and closing the plasmid. *SEC15b* was PCR amplified and cloned by *Bam*HI and *Xba*I enzymes into *pBAR* vector (kindly provided by Ben Holt, University of North Carolina). *pBAR1* was modified by inserting a *GFP* cassette for N-terminal fusions driven by the *35S* promoter (cloned from the *pCAT* vector) using *Hin*dIII and *Bam*HI sites. *EXO70A1* was amplified as cDNA bordered by *Spe*I sites and inserted into *Xba*I site of the *pBAR1*.

The native promoter-driven GFP-tagged SEC8 line was developed by adapting a *LAT52-SEC8* (Cole et al., 2005). A modified *GFP* coding sequence (Chiu et al., 1996) was inserted into the construct at the 5′ end of the *SEC8* sequence using *Bam*HI and *Afl*II. The *LAT52* promoter was excised by *Bam*HI and *Sal*I, and the presumptive promoter for *SEC8* (886 bp 5′ to the *SEC8* start codon) was amplified from the genomic sequence and ligated into its place. The *native promoter-GFP-SEC8* construct was verified by sequencing and transformed into *Arabidopsis* plants containing the *sec8-1* mutation (Cole et al., 2005). The function of the construct was verified by complementation of the pollen transmission defect normally associated with *sec8-1* (Kulich et al., 2010).

Arabidopsis plants were transformed by *Agrobacterium tumefaciens*–mediated transformation using the floral dip method (Clough and Bent, 1998).

Microscopy

Scanning electron micrographs were taken using JEOL JSM-6380LV (located at the Institute of Geology and Paleontology, Charles University, Prague) in the low vacuum regime.

For transmission electron microscopy, true leaves of 11-d-old seedlings were fixed for 24 h in 2.5% glutaraldehyde in 0.1 M cacodylate buffer, pH 7.2, and postfixed in 2% OsO_4 in the same buffer. Fixed tissue was dehydrated through an ethanol and acetone series and embedded in EponAraldite. Thin sections were cut on a Reichert-Jung Ultracut E ultramicrotome and stained using uranyl acetate and lead citrate. Sections were examined and photographed using a JEOL JEM-1011 electron microscope equipped with Veleta CCD camera Olympus Soft Imaging Solution software.

For live-cell imaging, the 4- to 7-d-old seedlings with the agar beneath them were transferred upside-down into a chambered cover glass (Lab-Tek II) and observed with Zeiss LSM 5 DUO confocal laser scanning microscope using the Zeiss C-Apochromat ×40/1.2 water corrected objective. For images in Figures 6A and 7C, the Live module was used.

FM4-64 (Invitrogen) was resuspended in DMSO to a concentration of 5 mM, diluted 1:1000 to 1:500 in water, and added into the chambered cover glass and incubated for 10 min prior to observation.

Accession Numbers

The accession numbers and T-DNA insertion lines used in this study are listed in Table 1.

ACKNOWLEDGMENTS

This work was supported by the Czech Ministry of Education (MSMT LC06034 and MSM0021620858), by KONTAKT ME10033, and by the Grant Agency of the Academy of Sciences of the Czech Republic (KJB600380806 and KJB600380802). The work in the lab of J.E.F. was supported by the U.S. National Science Foundation (IBN-0420226 and IOS-0920747), which also supported this international collaboration. We thank the Confocal Microscopy Facility of the Center for Genome Research and Biocomputing and the Environmental and Health Sciences Center at Oregon State University, which was supported in part by a grant from the National Institutes of Health (1S10RR107903-01). We also thank colleagues from the Faculty of Science at Charles University: Fatima Cvrčková for critical reading of the manuscript, Petr Jedelský for assistance with proteomic analysis, Martin Mazuch for scanning electron microscopy, and Roman Pleskot for the cell plate illustrations. M.F. would like to thank to developers of Ubuntu Linux, Gimp, and Inkscape.

Received January 29, 2010; revised August 25, 2010; accepted September 7, 2010; published September 24, 2010.

REFERENCES

Abramoff, M.D., Magelhaes, P.J., and Ram, S.J. (2004). Image Processing with ImageJ. Biophotonics Int. **11:** 36–42.

Buschmann, H., Chan, J., Sanchez-Pulido, L., Andrade-Navarro, M.A., Doonan, J.H., and Lloyd, C.W. (2006). Microtubule-associated AIR9 recognizes the cortical division site at preprophase and cell-plate insertion. Curr. Biol. **16:** 1938–1943.

Chiu, W., Niwa, Y., Zeng, W., Hirano, T., Kobayashi, H., and Sheen, J. (1996). Engineered GFP as a vital reporter in plants. Curr. Biol. **6:** 325–330.

Chow, C.M., Neto, H., Foucart, C., and Moore, I. (2008). Rab-A2 and Rab-A3 GTPases define a trans-Golgi endosomal membrane domain in *Arabidopsis* that contributes substantially to the cell plate. Plant Cell **20:** 101–123.

Clough, S.J., and Bent, A.F. (1998). Floral dip: A simplified method for *Agrobacterium*-mediated transformation of *Arabidopsis thaliana.* Plant J. **16:** 735–743.

Cole, R.A., Synek, L., Žárský, V., and Fowler, J.E. (2005). SEC8, a subunit of the putative *Arabidopsis* exocyst complex, facilitates pollen germination and competitive pollen tube growth. Plant Physiol. **138:** 2005–2018.

Croteau, N.J., Furgason, M.L.M., Devos, D., and Munson, M. (2009). Conservation of helical bundle structure between the exocyst subunits. PLoS ONE **4:** e4443.

Crowell, E.F., Bischoff, V., Desprez, T., Rolland, A., Stierhof, Y.D., Schumacher, K., Gonneau, M., Höfte, H., and Vernhettes, S. (2009). Pausing of Golgi bodies on microtubules regulates secretion of cellulose synthase complexes in *Arabidopsis.* Plant Cell **21:** 1141–1154.

Cutler, S.R., and Ehrhardt, D.W. (2002). Polarized cytokinesis in vacuolate cells of *Arabidopsis.* Proc. Natl. Acad. Sci. USA **99:** 2812–2817.

Dong, G., Hutagalung, A.H., Fu, C., Novick, P., and Reinisch, K.M. (2005). The structures of exocyst subunit Exo70p and the Exo84p C-terminal domains reveal a common motif. Nat. Struct. Mol. Biol. **12:** 1094–1100.

Eliáš, M., Drdová, E., Žiak, D., Bavlnka, B., Hála, M., Cvrčková, F., Soukupová, H., and Žárský, V. (2003). The exocyst complex in plants. Cell Biol. Int. **27:** 199–201.

Falbel, T.G., Koch, L.M., Nadeau, J.A., Seguí-Simarro, J.M., Sack, F.D., and Bednarek, S.Y. (2003). SCD1 is required for cytokinesis and polarized cell expansion in *Arabidopsis thaliana* [corrected]. Development **130:** 4011–4024.

Fielding, A.B., Schonteich, E., Matheson, J., Wilson, G., Yu, X., Hickson, G.R.X., Srivastava, S., Baldwin, S.A., Prekeris, R., and Gould, G.W. (2005). Rab11-FIP3 and FIP4 interact with Arf6 and the exocyst to control membrane traffic in cytokinesis. EMBO J. **24:** 3389–3399.

Finger, F.P., Hughes, T.E., and Novick, P. (1998). Sec3p is a spatial landmark for polarized secretion in budding yeast. Cell **92:** 559–571.

Gromley, A., Yeaman, C., Rosa, J., Redick, S., Chen, C.T., Mirabelle, S., Guha, M., Sillibourne, J., and Doxsey, S.J. (2005). Centriolin anchoring of exocyst and SNARE complexes at the midbody is required for secretory-vesicle-mediated abscission. Cell **123:** 75–87.

Grote, E., Carr, C.M., and Novick, P.J. (2000). Ordering the final events in yeast exocytosis. J. Cell Biol. **151:** 439–452.

Guo, W., Grant, A., and Novick, P. (1999a). Exo84p is an exocyst protein essential for secretion. J. Biol. Chem. **274:** 23558–23564.

Guo, W., Roth, D., Walch-Solimena, C., and Novick, P. (1999b). The exocyst is an effector for Sec4p, targeting secretory vesicles to sites of exocytosis. EMBO J. **18:** 1071–1080.

Guo, W., Tamanoi, F., and Novick, P. (2001). Spatial regulation of the exocyst complex by Rho1 GTPase. Nat. Cell Biol. **3:** 353–360.

Gutierrez, R., Lindeboom, J.J., Paredez, A.R., Emons, A.M.C., and Ehrhardt, D.W. (2009). *Arabidopsis* cortical microtubules position cellulose synthase delivery to the plasma membrane and interact with cellulose synthase trafficking compartments. Nat. Cell Biol. **11:** 797–806.

Hála, M., Cole, R., Synek, L., Drdová, E., Pečenková, T., Nordheim, A., Lamkemeyer, T., Madlung, J., Hochholdinger, F., Fowler, J.E., and Žárský, V. (2008). An exocyst complex functions in plant cell growth in *Arabidopsis* and tobacco. Plant Cell **20:** 1330–1345.

Hall, Q., and Cannon, M.C. (2002). The cell wall hydroxyproline-rich glycoprotein RSH is essential for normal embryo development in *Arabidopsis.* Plant Cell **14:** 1161–1172.

Hamburger, Z.A., Hamburger, A.E., West, A.P.J., Jr., and Weis, W.I. (2006). Crystal structure of the *S. cerevisiae* exocyst component Exo70p. J. Mol. Biol. **356:** 9–21.

Hazuka, C.D., Foletti, D.L., Hsu, S.C., Kee, Y., Hopf, F.W., and Scheller, R.H. (1999). The sec6/8 complex is located at neurite outgrowth and axonal synapse-assembly domains. J. Neurosci. **19:** 1324–1334.

Heese, M., Gansel, X., Sticher, L., Wick, P., Grebe, M., Granier, F., and Jürgens, G. (2001). Functional characterization of the KNOLLE-interacting t-SNARE AtSNAP33 and its role in plant cytokinesis. J. Cell Biol. **155:** 239–249.

Hsu, S.C., Hazuka, C.D., Roth, R., Foletti, D.L., Heuser, J., and Scheller, R.H. (1998). Subunit composition, protein interactions, and structures of the mammalian brain sec6/8 complex and septin filaments. Neuron **20:** 1111–1122.

Jürgens, G. (2005). Plant cytokinesis: Fission by fusion. Trends Cell Biol. **15:** 277–283.

Karimi, M., Inzé, D., and Depicker, A. (2002). GATEWAY vectors for *Agrobacterium*-mediated plant transformation. Trends Plant Sci. **7:** 193–195.

Koumandou, V.L., Dacks, J.B., Coulson, R.M.R., and Field, M.C. (2007). Control systems for membrane fusion in the ancestral eukaryote; evolution of tethering complexes and SM proteins. BMC Evol. Biol. **7:** 29.

Kulich, I., Cole, R., Drdová, E., Cvrčková, F., Soukup, A., Fowler, J., and Žárský, V. (2010). Arabidopsis exocyst subunits SEC8 and EXO70A1 and exocyst interactor ROH1 are involved in the localized deposition of seed coat pectin. New Phytol., in press.

Lauber, M.H., Waizenegger, I., Steinmann, T., Schwarz, H., Mayer, U., Hwang, I., Lukowitz, W., and Jürgens, G. (1997). The *Arabidopsis* KNOLLE protein is a cytokinesis-specific syntaxin. J. Cell Biol. **139:** 1485–1493.

Lavy, M., Bloch, D., Hazak, O., Gutman, I., Poraty, L., Sorek, N., Sternberg, H., and Yalovsky, S. (2007). A Novel ROP/RAC effector links cell polarity, root-meristem maintenance, and vesicle trafficking. Curr. Biol. **17:** 947–952.

Martín-Cuadrado, A.B., Morrell, J.L., Konomi, M., An, H., Petit, C., Osumi, M., Balasubramanian, M., Gould, K.L., Del Rey, F., and de Aldana, C.R.V. (2005). Role of septins and the exocyst complex in the function of hydrolytic enzymes responsible for fission yeast cell separation. Mol. Biol. Cell **16:** 4867–4881.

Matar, D., and Catesson, A.M. (1988). Cell plate development and delayed formation of the pectic middle lamella in root meristems. Protoplasma **146:** 10–17.

Mineyuki, Y., and Gunning, B. (1990). A role for preprophase bands of microtubules in maturation of new cell-walls, and a general proposal on the function of preprophase band sites in cell-division in higher-plants. J. Cell Sci. **97:** 527–537.

Moskalenko, S., Tong, C., Rosse, C., Mirey, G., Formstecher, E., Daviet, L., Camonis, J., and White, M.A. (2003). Ral GTPases regulate exocyst assembly through dual subunit interactions. J. Biol. Chem. **278:** 51743–51748.

Munson, M., and Novick, P. (2006). The exocyst defrocked, a framework of rods revealed. Nat. Struct. Mol. Biol. **13:** 577–581.

Nakagawa, T., Kurose, T., Hino, T., Tanaka, K., Kawamukai, M., Niwa, Y., Toyooka, K., Matsuoka, K., Jinbo, T., and Kimura, T. (2007). Development of series of gateway binary vectors, pGWBs, for realizing efficient construction of fusion genes for plant transformation. J. Biosci. Bioeng. **104:** 34–41.

Novick, P., Field, C., and Schekman, R. (1980). Identification of 23 complementation groups required for post-translational events in the yeast secretory pathway. Cell **21:** 205–215.

Otegui, M.S., Mastronarde, D.N., Kang, B.H., Bednarek, S.Y., and Staehelin, L.A. (2001). Three-dimensional analysis of syncytial-type cell plates during endosperm cellularization visualized by high resolution electron tomography. Plant Cell **13:** 2033–2051.

Otegui, M.S., and Staehelin, L.A. (2004). Electron tomographic analysis of post-meiotic cytokinesis during pollen development in *Arabidopsis thaliana.* Planta **218:** 501–515.

Otegui, M.S., Verbrugghe, K.J., and Skop, A.R. (2005). Midbodies and phragmoplasts: Analogous structures involved in cytokinesis. Trends Cell Biol. **15:** 404–413.

Reichelt, S., Knight, A.E., Hodge, T.P., Baluška, F., Šamaj, J., Volkmann, D., and Kendrick-Jones, J. (1999). Characterization of the unconventional myosin VIII in plant cells and its localization at the post-cytokinetic cell wall. Plant J. **19:** 555–567.

Rosso, M.G., Li, Y., Strizhov, N., Reiss, B., Dekker, K., and Weisshaar, B. (2003). An *Arabidopsis thaliana* T-DNA mutagenized population (GABI-Kat) for flanking sequence tag-based reverse genetics. Plant Mol. Biol. **53:** 247–259.

Samuel, M.A., Chong, Y.T., Haasen, K.E., Aldea-Brydges, M.G., Stone, S.L., and Goring, D.R. (2009). Cellular pathways regulating responses to compatible and self-incompatible pollen in *Brassica* and *Arabidopsis* stigmas intersect at Exo70A1, a putative component of the exocyst complex. Plant Cell **21:** 2655–2671.

Samuels, A.L., Giddings, T.H.J., Jr., and Staehelin, L.A. (1995). Cytokinesis in tobacco BY-2 and root tip cells: a new model of cell plate formation in higher plants. J. Cell Biol. **130:** 1345–1357.

Seguí-Simarro, J.M., Austin II, J.R.I.I., White, E.A., and Staehelin, L.A. (2004). Electron tomographic analysis of somatic cell plate formation in meristematic cells of *Arabidopsis* preserved by high-pressure freezing. Plant Cell **16:** 836–856.

Sessions, A., et al. (2002). A high-throughput *Arabidopsis* reverse genetics system. Plant Cell **14:** 2985–2994.

Sivaram, M.V.S., Furgason, M.L.M., Brewer, D.N., and Munson, M. (2006). The structure of the exocyst subunit Sec6p defines a conserved architecture with diverse roles. Nat. Struct. Mol. Biol. **13:** 555–556.

Smith, T.J., and Bell, J.E. (1986). An exponential gradient marker for use with minigel polyacrylamide electrophoresis systems. Anal. Biochem. **152:** 74–77.

Synek, L., Schlager, N., Eliáš, M., Quentin, M., Hauser, M.T., and Žárský, V. (2006). AtEXO70A1, a member of a family of putative exocyst subunits specifically expanded in land plants, is important for polar growth and plant development. Plant J. **48:** 54–72.

TerBush, D.R., Maurice, T., Roth, D., and Novick, P. (1996). The Exocyst is a multiprotein complex required for exocytosis in *Saccharomyces cerevisiae.* EMBO J. **15:** 6483–6494.

TerBush, D.R., and Novick, P. (1995). Sec6, Sec8, and Sec15 are components of a multisubunit complex which localizes to small bud tips in *Saccharomyces cerevisiae.* J. Cell Biol. **130:** 299–312.

Van Damme, D., Coutuer, S., De Rycke, R., Bouget, F.Y., Inzé, D., and Geelen, D. (2006). Somatic cytokinesis and pollen maturation in *Arabidopsis* depend on TPLATE, which has domains similar to coat proteins. Plant Cell **18:** 3502–3518.

Verma, D.P. (2001). Cytokinesis and building of the cell plate in plants. Annu. Rev. Plant Physiol. Plant Mol. Biol. **52:** 751–784.

Walker, K.L., Müller, S., Moss, D., Ehrhardt, D.W., and Smith, L.G. (2007). *Arabidopsis* TANGLED identifies the division plane throughout mitosis and cytokinesis. Curr. Biol. **17:** 1827–1836.

Wang, H., Tang, X., Liu, J., Trautmann, S., Balasundaram, D., McCollum, D., and Balasubramanian, M.K. (2002). The multiprotein exocyst complex is essential for cell separation in *Schizosaccharomyces pombe.* Mol. Biol. Cell **13:** 515–529.

Wen, T.J., Hochholdinger, F., Sauer, M., Bruce, W., and Schnable, P.S. (2005). The *roothairless1* gene of maize encodes a homolog of *sec3*, which is involved in polar exocytosis. Plant Physiol. **138:** 1637–1643.

Wu, S., Mehta, S.Q., Pichaud, F., Bellen, H.J., and Quiocho, F.A. (2005). Sec15 interacts with Rab11 via a novel domain and affects Rab11 localization in vivo. Nat. Struct. Mol. Biol. **12:** 879–885.

Yang, M., Nadeau, J.A., Zhao, L., and Sack, F.D. (1999). Characterization of a cytokinesis defective (cyd1) mutant of *Arabidopsis.* J. Exp. Bot. **50:** 1437–1446.

Zajac, A., Sun, X., Zhang, J., and Guo, W. (2005). Cyclical regulation of the exocyst and cell polarity determinants for polarized cell growth. Mol. Biol. Cell **16:** 1500–1512.

Žárský, V., Cvrčková, F., Potocký, M., and Hála, M. (2009). Exocytosis and cell polarity in plants: Exocyst and recycling domains. New Phytol. **183:** 255–272.

Zhang, X., Bi, E., Novick, P., Du, L., Kozminski, K.G., Lipschutz, J.H., and Guo, W. (2001). Cdc42 interacts with the exocyst and regulates polarized secretion. J. Biol. Chem. **276:** 46745–46750.

Zhang, X., Wang, P., Gangar, A., Zhang, J., Brennwald, P., TerBush, D., and Guo, W. (2005a). Lethal giant larvae proteins interact with the exocyst complex and are involved in polarized exocytosis. J. Cell Biol. **170:** 273–283.

Zhang, X., Zajac, A., Zhang, J., Wang, P., Li, M., Murray, J., TerBush, D., and Guo, W. (2005b). The critical role of Exo84p in the organization and polarized localization of the exocyst complex. J. Biol. Chem. **280:** 20356–20364.